Raman spectrum of the superconductor $Bi_2Sr_2CaCu_2O_8$

J. Sapriel, L. Pierre, D. Morin, J. C. Toledano, J. Schneck, H. Savary, J. Chavignon, J. Primot, C. Daguet, and J. Etrillard
Centre National d'Études des Telecommunications, 196 rue Henri Ravera 92220, Bagneux, France

H. Boyer
Instrument S. A. Jobin-Yvon Division BP118 Longjumeau Cedex, France
(Received 12 August 1988)

Two Raman setups, one with high resolution, and the other for spatially resolved (1×1 μm^2) experiments, have been used to investigate the polarized Raman spectra of a superconducting single crystal of the (2:2:1:2) phase $Bi_2Sr_2CaCu_2O_8$, and the unpolarized micro-Raman spectra of three ceramics, two of which have zero resistance below $\sim$105 K and contain substantial proportions of the (2:2:2:3) phase ($\sim$15%–20%). Our spectra differ in some aspects from those recently published for the (2:2:1:2) phase. The occurrence of several low-frequency lines ($\nu \leq 65$ cm^{-1}) is confirmed. The width of the lines and their shape is discussed with regard to the occurrence of disorder in the structure and of an electron-phonon coupling. The spectra of the ceramics reveal the presence of four minority phases in addition to the main phases (2:2:1:2) and (2:2:2:3). The ceramics containing the (2:2:2:3) phase display the same lines as the ceramic not containing this phase. This result is discussed in the light of the structural information available and of the grain-growth habit of the (2:2:1:2) phase.

In the high-T_c superconductors, a large number of Raman scattering studies have been reported, aimed at clarifying the characteristics of the phonon structure of the materials considered. These studies have attempted to draw from the results a variety of information on the physical properties of the materials, which are more or less directly related to the mechanism of superconductivity.

For instance, in the case of $YBa_2Cu_3O_7$, the Raman scattering technique (with or without a microprobe setup) has been used in order to investigate the nature of the phases present in ceramics,[1] the dependence of the phonon spectrum on the oxygen content,[2] the consistency of the observed spectrum with lattice force models,[3] the anisotropy of the structure,[4] and the occurrence of structural transitions.[5] Recently, the Raman spectrum of $YBa_2Cu_3O_7$ has also been claimed[6] to contain features of central importance to the understanding of the mechanism of high-T_c superconductivity, such as evidence of a strong electron-phonon coupling, of the existence of a superconductivity gap, and of a small residual density of electronic states within this gap.

In the present paper, we examine some of the former problems, in the case of the bismuth-containing class of high-T_c superconductors.[7] We describe and discuss two main sets of experimental results. First, we consider the Raman spectra of a homogeneous single crystal of the (2:2:1:2) superconducting phase. Second, we investigate the spatially resolved, micro-Raman spectra of three ceramics, two of which display zero resistance below $\sim$105 K and contain a substantial (15%–20%) fraction of the (2:2:2:3) phase.

In the bismuth-containing family of compounds, two prominent high-T_c superconducting phases have been distinguished. One, labeled (2:2:1:2), of approximate formula $Bi_2Sr_2CaCu_2O_{8+x}$ has zero resistance below $\sim$65–75 K. The other, labeled (2:2:2:3), of formula $Bi_2Sr_2Ca_2Cu_3O_{10+x}$ has zero resistance below $\sim$102–107 K. The structures of these two phases are not entirely elucidated at present. In a first approximation,[8] both phases can be considered tetragonal. Their space group is $I4/mmm$, and the primitive unit cell contains a single formula (the tetragonal multiple cell contains two formulas) (Fig. 1).

Refinement of the structure of the (2:2:1:2) phase[9] has shown that a better approximation of the structure may be associated with a one-face centered orthorhombic Bravais lattice with two formulas per primitive unit cell. It has also been found that a modulation is superimposed on this approximate structure. Its **k** vector has an incommensurate component along the *b*-orthorhombic axis. Substantial disorder between the strontium and calcium sites affects the structure.[10] As for the (2:2:2:3) phase, it is known to be orthorhombic and (possibly) incommensurate,[11] with a structure closely related to that of the (2:2:1:2) phase (Fig. 1).

Four Raman studies of the bismuth-containing superconductors have recently been reported. Two[12,13] concern the spectra of ceramics mainly containing phases distinct from the two above-mentioned phases of interest. In one of these works,[13] two Raman lines relative to the (2:2:1:2) phase are specified.

The Raman spectrum of the (2:2:1:2) phase has been analyzed in a more complete way by Cardona *et al.*[14] and by Farrow *et al.*[15] Both papers indicate the results of a normal-mode analysis respectively based on the refined orthorhombic structure, and on the tetragonal approximate structure. Cardona *et al.* have analyzed a "highly oriented polycrystal," while Farrow *et al.* have investigated a single crystal involving substantial inhomogeneities.[15] The spectra obtained in these two papers present major

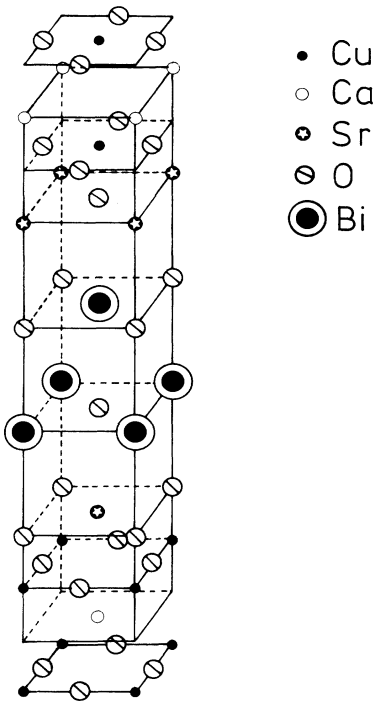

FIG. 1. Approximate structures, with tetragonal *I*4/*mmm* symmetry, of the (2:2:1:2) and (2:2:2:3) phases. Half of the tetragonal cell is represented. The upper and lower CuO_2 planes belong to the (2:2:2:3) phase only, while the remaining structure is common to the two phases.

differences.

Our work has in common with these two papers a comprehensive investigation of the room-temperature Raman spectrum of the (2:2:1:2) phase. We have used a single crystal with good compositional homogeneity, which displayed a uniform Raman spectrum across the surface (using a micron-sized probe). We have given special attention to a comparison of the single-crystal spectrum with those of ceramics, as well as to the characteristics of the Raman lines profiles.

Single crystals of the (2:2:1:2) phase were obtained by slowly cooling a melt of composition ($Bi_2Sr_2CaCu_2O_8$ +7CuO). Platelets, $\sim$100-μm thick, and several mm in lateral size were extracted from the solidified melt. X-ray analysis showed that these platelets were composed of thin ($\sim$10 μm) single-crystalline wafers, normal to the *c* axis, possessing a diffraction pattern characteristic of the (2:2:1:2) phase ($a\sim b\sim 5.4$ Å, $c\sim 30.7$ Å; and series of satellite reflections along *b*, associated to an incommensurate modulation). The platelet selected for the Raman experiment was triangular shaped and $\sim$1 mm in size. Its crystallographic axes were identified as the extinction directions in reflected polarized light as well as by means of an x-ray precession camera. The latter technique showed modulation satellites along two perpendicular directions, thus revealing a twinning of the plate corresponding to the coexistence of regions differing by the interchange of the *a* and *b* axes. This plate was submitted to an electron-microprobe chemical analysis. Scanning the probe across the surface showed that, at a spatial resolution of a few microns, the surface of the plate had the uniform composition $Bi_2Sr_{2.1}Ca_{0.8}Cu_{1.85}O_x$, close to the nominal composition of the (2:2:1:2) phase. Electrical measurements yielded a resistive transition with an onset of $\sim$85 K, and zero resistance below $\sim$65 K.

Three ceramics which we denote a, b, and c were examined. They were prepared according to a method described elsewhere,[16] from the starting composition $Bi_{1.8}Pb_{0.2}Sr_2Ca_2Cu_3O_{10}$. The phases present in each one were determined by means of x-ray powder diffraction, resistivity, and magnetic-susceptibility measurements. These methods will not detect phases which are in too small proportions (i.e., a few percent) or not superconducting. Ceramic a was found to contain the (2:2:1:2) phase with orthorhombic lattice constants $a\sim b\sim 5.4$ Å and $c\sim 30.7$ Å. Ceramics a and c contain two dominant phases, the (2:2:1:2) phase, and 15–20% of the (2:2:2:3) phase with lattice constants $a\sim 5.4$ and $c\sim 37$ Å. The two latter ceramics were observed to possess zero resistance below $\sim$105 K. This temperature varied by a few degrees, depending critically on the current used for the measurement, in accordance with the proportion of the (2:2:2:3) phase, close to the three-dimensional percolation threshold.

Two different Raman setups were used. One was only applied to the single-crystal analysis. The second was used for both the ceramic and single-crystal work. In the first setup, the single-crystal was placed in vacuum, in order to avoid superposition of light scattering by the air. 50 mW of a 5145-Å laser beam were focused on an elliptic spot (25×50 μm^2) on the (001)-oriented surface of the sample. The beam was kept at an almost grazing incidence ($\sim$70° of the normal) and the scattered light was collected in the direction of the normal to the sample. This geometry has the advantage of minimizing the stray light. Due to the high refractive index of the material considered, the incident light propagates, within the sample, close to the normal to the surface (i.e., the *c* direction) and the scattering geometry is therefore equivalent to a backscattering one. The scattered light was analyzed by means of a Jobin & Yvon U1000 spectrometer involving a double monochromator having high transmission, high contrast (10^{-14} stray light at 20 cm^{-1}), and high dispersion (9 cm^{-1}/mm), and is well adapted to the study of the line profiles of the low-frequency part of the spectrum. Due to the weakness of the scattered light a scan up to $\sim$800 cm^{-1} required 8 h. Typical intensities of the lines were a few thousand counts/minute for a resolution of $\sim$3 cm^{-1}.

The second setup was a micro-Raman probe based on the Jobin & Yvon S3000 double monochromator, allowing a spatial resolution of 1×1 μm^2. In this setup the laser power focused on the sample was limited to 1 mW and the geometrical configuration used was a regular backscattering one. Due to the use of a multichannel detection, complete scans, between 85 and 650 cm^{-1}, could be performed much more rapidly than in the first setup (20 min).

In the same manner as Farrow *et al.*,[15] we refer the lat-

tice dynamics of the (2:2:1:2) and (2:2:2:3) phases to the approximate tetragonal structure represented in Fig. 1. The use of a more complex structural information appears superfluous in a first step of the analysis. Indeed, the actual structures (whose features are yet to be confirmed) only differ by slight atomic shifts from the simplified structures. Accordingly, we expect that the deviations from the tetragonal symmetry will give rise to small effects in the Raman spectra (i.e., splittings of the order of a few wave numbers or weak additional lines), which are probably not easily accessible with the small size and the wafer morphology of the currently available crystals.

The approximate tetragonal structures of the (2:2:1:2) and (2:2:2:3) phases possess, respectively, 15 and 19 atoms (i.e., one formula) in the primitive unit cell.

Decomposition into normal modes with $\mathbf{k}=0$, of the oscillations of the atoms about their equilibrium positions, can be performed easily for the two symmorphic structures in Fig. 1. The (2:2:1:2) structure has 14 infrared active modes $(6A_u+B_{1u}+7E_u)$ and 14 Raman-active modes $(6A_g+B_{1g}+7E_g)$. The notation used is the same as Farrow's,[15] A_g is a totally symmetric mode, B_{1g} and E_g describe, respectively, the symmetries of the second-rank tensor components $(XX\text{-}YY)$, and (XZ,YZ) referred to the tetragonal axes. Likewise, the decomposition relative to the (2:2:2:3) structure yields 20 infrared active modes $(8A_u+2B_{1u}+10E_u)$ and 16 Raman active modes $(7A_g+B_{1g}+E_g)$.

The c-backscattering configuration used in the single-crystal study does not allow the detection of the E_g modes for which either the incident or the scattered polarization should be parallel to c. Therefore, a maximum of 7 modes are expected to be observed for the (2:2:1:2) phase. In principle, the experimental constraints are looser for ceramics. However, as explained below, the morphology of the ceramic grains as well as the high-refractive index of the materials determine the same qualitative spectrum for a ceramic and a c-oriented crystalline plate.

The A_g modes of the (2:2:1:2) structure are combinations of motions, parallel to the c axis, of all the atoms in the structure except the calcium ones.[15] The B_{1g} mode concerns the oxygen atoms labeled O(1) lying in the copper planes.[8] In the (2:2:2:3) structure, the additional A_g mode arises from the fact that the calcium atoms contribute to the formation of the Raman-active modes while their motion is Raman inactive in the (2:2:1:2) structure. Note also that the additional copper-oxygen plane of the (2:2:2:3) phase only gives rise to the infrared active modes.

Let us consider the Raman spectra of the (2:2:1:2) phase which are deduced from the single-crystal data. A plot of the spectrum, up to 800 cm^{-1}, is shown on Fig. 2. Figure 3 reproduces the details of the spectrum below 70 cm^{-1}. We observe 8 lines whose frequencies and width are listed in Table I. In this table, we have also listed the lines assigned to the (2:2:1:2) phase in Refs. 14 and 15.

Several aspects are of interest in the description and analysis of the experimental results.

First, it is relevant to compare our data to the ones in Refs. 14 and 15, and discuss the validity of the correspondence between the lines observed and the

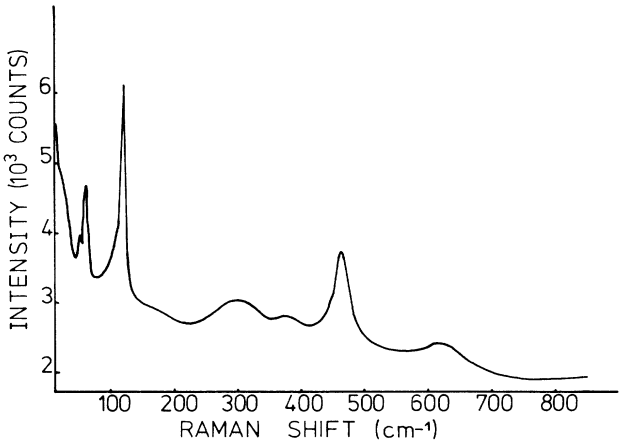

FIG. 2. Plot of the room-temperature Raman spectrum of the (2:2:1:2) single crystal corresponding to phonons of A_g symmetry propagating along c. The polarizations for the incident and scattered beams are parallel to each other and parallel to the orthorhombic axes a or b; 50 mW of the incident laser beam ($\lambda=5145$ Å) are directed at grazing incidence and focused on a 25×50 μm^2 spot on the (001) oriented surface of the sample. No Raman signal has been observed for crossed polarizations of the incident and scattered light beams.

(2:2:1:2) phase.

The lines composing our Raman data above 100 cm^{-1} appear as a subset of the lines observed by Cardona *et al.*[14] (*C*), while they differ very significantly from the spectrum described by Farrow *et al.*[15] (*F*). Below 100 cm^{-1} no lines were detected by *C*. We observed three low-frequency lines, one of which can be identified as a line reported by *F*.

On the basis of Table I, three lines can be unambiguously assigned to the (2:2:1:2) phase, respectively located, in our spectra, at 61 ± 2 cm^{-1}, 118 ± 2 cm^{-1}, and 463 ± 3 cm^{-1}. They possess significantly higher intensity than the remaining spectrum. Besides, their relevance is

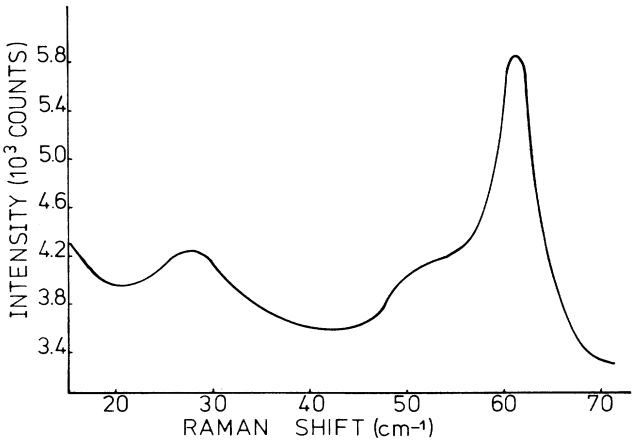

FIG. 3. Plot of the Raman spectrum of a (2:2:1:2) single crystal in the frequency range below 70 cm^{-1} with the same experimental conditions as in Fig. 2.

TABLE I. Frequencies of the Raman spectra observed in a single crystal of the (2:2:1:2) phase in Refs. 14 and 15 as well as in the present work. Bracketed numbers indicate weaker lines. The asterisks show the lines which are assigned to the intrinsic first-order spectrum of the (2:2:1:2) phase.

Mode frequencies		Present work	
Ref. 14 (cm^{-1})	Ref. 15 (cm^{-1})	Frequency (cm^{-1})	Width (cm^{-1})
		27.5 ± 2*	8
		51.5 ± 2*	9
	64*	61 ± 2*	6
	98		
122*	129*	118 ± 2*	8
(133)			
(156)	(148)		
184			
(219)	(220)		
282*		(300 ± 10)*	
296			. . .
313			
	(347)		
(391)		(385 ± 10)	. . .
469*	461*	463 ± 3*	20
	497		
631*		(620 ± 10)*	
659			. . .

supported by the results of *C* and *F*. The first line is located close to the 64-cm^{-1} line displayed by the spectrum in *F*. The line at 118 cm^{-1} matches the intense lines detected at 122 cm^{-1} in *C* and at 129 cm^{-1} in *F*. Likewise, a strong line is observed in the vicinity of $\sim$460 cm^{-1} by *F* and *C*, as well as by Hadjiev and Iliev.[13]

Below 100 cm^{-1}, *F* point out the existence of an additional low-frequency line at $\sim$98 cm^{-1}, which has higher intensity than the 64-cm^{-1} line. This line probably belongs to the Raman spectrum of a different phase. Indeed, we find no trace of a signficant scattering in our spectra, in the neighborhood of the above frequency, while the counterpart of the 64-cm^{-1} line is clearly observed. The fact that a single crystal of the (2:2:1:2) phase may contain significant amounts of impurity phases has been noted by Tarascon *et al.*[17] for samples of the same origin as used by *F*. More precisely, the 98-cm^{-1} line may be related to the presence of the phase $Bi_2CaSr_3O_x$, which has been found[13] as a residual phase in Bi-Sr-Ca-Cu-O ceramics, and which is known to possess[13] an intense and sharp Raman line at $\sim$90–93 cm^{-1}.

In the low-frequency range (Fig. 2), we find two weaker lines at 51.5 ± 2 cm^{-1} and at 27.5 ± 2 cm^{-1}. We have checked conclusively their occurrence by probing several regions of the crystal. Note that these lines were only detected in the high-resolution Raman setup involving a scattering geometry minimizing the stray light. Accordingly, they might have escaped earlier investigations performed in a regular backscattering geometry.

Aside from the lines already discussed, the spectrum described by *F* contains 3 weak lines and one strong line at 497 cm^{-1}. This line has no counterpart in our spectra or in the results of *C*. In the range above 120-cm^{-1} frequencies, we observe three broad structures centered at 300 ± 10 cm^{-1}, 385 ± 10 cm^{-1}, and 620 ± 10 cm^{-1}. These structures are also reported by *C* at slightly shifted locations. The latter one, at $\sim$620–630 cm^{-1}, has been observed with similar frequencies, in every phase of the same structural family.[12,13] It is therefore likely to represent the oscillation of a basic structural feature of this family (e.g., a motion of the perovskitelike structural elements).

To sum-up the above discussion, the (2:2:1:2) phase can be put in correspondence with all the eight lines present in our spectra. Six of these lines at 27, 51, 61, 118, 463, and 620 cm^{-1} have significant intensities and separation, and a relatively small width. They are unlikely to arise either from a small deviation from tetragonality or from a second-order process. Accordingly, we can assign them, with some confidence, to the first-order Raman spectrum of the approximate tetragonal structure of the (2:2:1:2) phase, represented in Fig. 1.

As argued hereafter, the seventh line expected on the basis of the normal mode analysis, is likely to be part of the broad structure at $\sim$300 cm^{-1}.

All the lines of the spectrum displayed in Figs. 2 and 3 behave as A_g symmetry lines. They are visible when the incident and the scattered beams have their polarizations parallel to each other, and parallel to the orthorhombic axis *a* or *b* (the two axes are not distinguished due to the twinning mentioned above). By contrast, these lines are extinguished when the two beams have crossed polarizations [i.e., in the $z(xy)\bar{z}$ geometry], the coordinates being referred to the orthorhombic axes *a*, *b*, *c*, the axes *a*, *b*, being tilted by 45° with respect to the tetragonal axes *X*, *Y*, in the *XY* plane. *C* have observed, in the same $z(xy)\bar{z}$ geometry, the persistence of a line at $\sim$280 cm^{-1}, which they associate with the B_{1g} mode expected on the basis of the normal-mode analysis. In our spectra, this frequency falls within the broad structure centered on $\sim$300 cm^{-1}. This structure has weaker intensity than its counterpart in Ref. 14. Its presence in the $x(xy)\bar{z}$ geometry might therefore have escaped our measurements. Note that *C* also point out the occurrence of a pronounced difference between the spectra obtained in the $z(xx)\bar{z}$ and the $z(yy)\bar{z}$ geometries. Such an anisotropy does not seem consistent with the fact that the samples used by these authors are polycrystals only having a common *c* orientation, and disordered orientations in the *a*-*b* plane.

A speculative assignment of the Raman lines to atomic motions, based on a comparison to the spectrum of $YBa_2Cu_3O_7$ (1:2:3), has been discussed by *C* and *F*. In contrast to these authors, we think that this comparison is only of interest to identify the lines associated with the motion of the copper-oxygen planes, since these are the only structural elements having the same chemical nature and a similar environment in the (1:2:3) and (2:2:1:2) compounds. In both materials, the copper-oxygen planes are associated with three Raman-active modes accessible in a *c*-backscattering experiment ($2A_g + B_{1g}$). There is agreement on the assignment of two of these modes, in the (1:2:3) compound, to lines located at $\sim$337 cm^{-1} (B_{1g})

and $\sim 440\ cm^{-1}$ (A_g). Depending on the authors, the third (1:2:3) mode is assigned either to a line at $\sim 220\ cm^{-1}$,[15] or to a line at $116\ cm^{-1}$.[6] The latter assignment seems more consistent with line-shape analysis.[6] Using the fact that the corresponding modes of the (2:2:1:2) structure should be located at similar frequencies, we can assign the motion along c of the atoms in the copper-oxygen planes to the lines observed in the (2:2:1:2) crystals, at $\sim 118\ cm^{-1}$ (A_g), and $463\ cm^{-1}$ (A_g), and to the broad structure at $\sim 300\ cm^{-1}$ (B_{1g}). For the first two lines, this assignment is consistent with the fact that in the two compounds, the corresponding lines have relatively large intensities. By contrast, the $337\text{-}cm^{-1}$ line is the dominant line of the (1:2:3) spectrum, while the $300\text{-}cm^{-1}$ line is a weak contribution to the (2:2:1:2) spectrum. An explanation of this difference resides in the occurrence of a pronounced "buckling" of the O—Cu—O bonds, in the (1:2:3) compound, while such a buckling is small in the (2:2:1:2) structure.[9] The presence of the buckling will determine a more efficient coupling between the motion of the oxygen atoms along c (i.e., the B_{1g} mode) and the light-beam polarized in the (x,y) plane, consistently with the higher intensity of the Raman line of the (1:2:3) compound.

Unlike F and C, we find no correspondence between the remaining lines of the (2:2:1:2) spectrum (at ~ 28, 51, 61, and $620\ cm^{-1}$) and lines observed in $YBa_2Cu_3O_7$, in accordance with the significant differences of the two structures. Moreover, the assignment of the low-frequency lines to definite atomic planes seems irrelevant. Such low frequencies are likely to be associated to "external" modes involving long-range interactions between the planes. The mass of the bismuth atom may, however, be partly responsible for the low frequencies observed.

Consider now the profiles of the lines associated to the atomic motions in the copper-oxygen plane. In $YBa_2Cu_3O_7$, the corresponding lines were shown[6] to have a characteristic asymmetric "Fano-shape" which was interpreted by Cooper *et al.*[6] as the result of a coupling between the considered lattice modes and the continuum of electronic excitations. Below the superconducting transition, the Fano asymmetry was found to be strongly attenuated, in accordance with a reduction of the density of electronic states. This reduction was assigned[6] to the opening of the superconductivity gap.

Since the electronic carriers are currently believed to lie within the CuO_2 planes in, both the (1:2:3) and (2:2:1:2) phases, it is of interest to find out if similar Fano asymmetries occur in the Raman spectrum of the (2:2:1:2) phase. Figure 4 reproduces a plot of the line at $118\ cm^{-1}$ relative to the (2:2:1:2) phase, as well as the corresponding line relative to the (1:2:3) phase. The latter spectrum has been obtained in the same experimental conditions as specified above on an $YBa_2Cu_3O_7$ single-crystal growth in our laboratory.[18] The instrumental resolution was similar ($\sim 4\ cm^{-1}$) to the one used in the case of the (2:2:1:2) single crystal. Figure 4 reveals a very striking difference between the two lines. In the (1:2:3) compound, our measurements yield a frequency ($\sim 110\ cm^{-1}$) which is slightly shifted with respect to the results of Cooper *et al.*,[6] but they confirm clearly the presence of the asymmetric Fano shape pointed out by these authors. The width of the line is $\sim 20\ cm^{-1}$. By contrast, the line observed in the (2:2:1:2) crystal is relatively narrow ($8\ cm^{-1}$) and its shape appears symmetric. No Fano-type asymmetry is noted either in the line at $463\ cm^{-1}$ (Fig. 5) and in the remaining lines of the spectrum (Figs. 2 and 3).

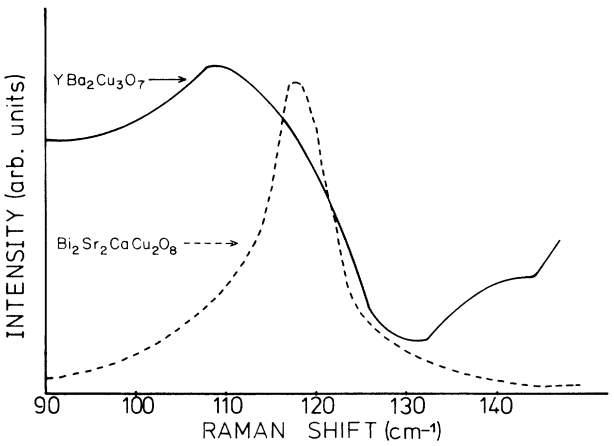

FIG. 4. Compared profiles of the Raman lines at 110–120 cm^{-1} in the (1:2:3) and (2:2:1:2) superconducting crystals, showing the absence of asymmetry in the bismuth-containing phase. Same experimental conditions as in Fig. 2.

This result does not rule out the presence of an electron-phonon coupling. Indeed, it is worth pointing out that, even if a similar electron-phonon coupling were present in the two considered materials, the absence of its manifestation in the Raman spectrum of the (2:2:1:2) phase can be understood. In this view, we can invoke again the absence of pronounced buckling of the oxygen-copper bonds in the latter phase. One can expect that carriers confined to the CuO_2 planes will interact essentially with atomic motions within these planes. In the (1:2:3)

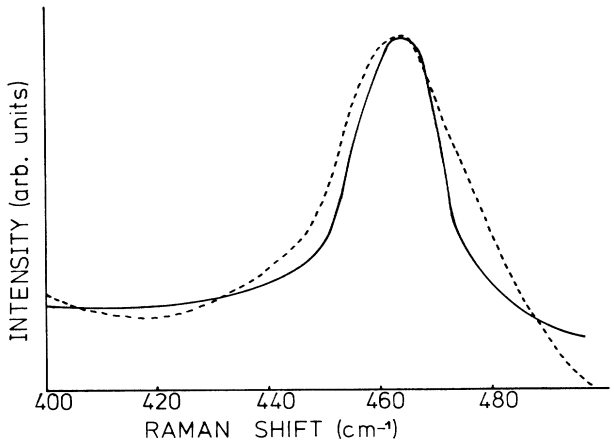

FIG. 5. Profile of the Raman $463\ cm^{-1}$ line relative to the A_g spectrum of the (2:2:1:2) phase. The two plots correspond to the probing of two different areas of the crystal surface. Same experimental conditions as in Fig. 2.

compound the buckling of the bonds will transfer part of this interaction to the *c*-polarized motions which are accessible to the *c*-backscattering Raman measurements. In the (2:2:1:2) compound such a transfer will be very small due to the absence of pronounced buckling. In order to reveal the possible existence of a Fano effect in the (2:2:1:2) phase it would be necessary to use a scattering geometry allowing to probe the E_g modes, since these modes essentially concern atomic motions within the *a-b* plane.

Let us now examine the Raman data obtained in the ceramics. As mentioned above, the three investigated ceramics contained some lead which has been substituted[16] for the bismuth constituent. This substitution has been effected in order to stabilize a substantial fraction of the (2:2:2:3) phase. For the (2:2:1:2) phase present in the ceramics, x-ray and electrical measurements[16] showed no significant variations of the lattice constants, or of the critical temperature (onset at $\sim$85 K), with respect to the values in the lead-free ceramics. The substitution is unlikely either to modify the lattice dynamics of the considered phases since the masses of the Bi and Pb atoms (209 and 207, respectively) differ by less than 1%.

Scanning the Raman microprobe on each of the three ceramics, we have detected four types of spectra. At most points investigated, in each ceramic, the spectrum obtained resembles closely the single-crystal spectrum assigned to the (2:2:1:2) phase.

The three other spectra, which are clearly different from the preceding one, and from each other, have been obtained a few times each on scanning the ceramics. We were able to assign these spectra to impurity phases. No trace of such impurity phases has been found in the x-ray Debye-Scherrer diagram of the same ceramics.[16] This puts an upper limit of a few percent for the fraction of the ceramic volume occupied by an impurity phase. The greater sensitivity of the micro-Raman technique is due to the fact that a phase will be detected, and its spectrum isolated, provided that the ceramic contains grains of this phase with dimensions comparable with the size of the focused beam (~ 1 μm).

The most intense lines of the spectra of the three minority phases are indicated in Table II. In order to identify these spectra, we have relied on the recent work of Hadjiev and Iliev.[13] These authors have assigned the Raman spectrum of various impurity phases of Bi-Sr-Ca-Cu-O ceramics by combining micro-Raman measurements with a local chemical analysis by means of scanning electron microscopy. Their results confirm earlier electron-microscopic and x-ray data by Hazen *et al.*[19] and by Tarascon *et al.*[17] Our measurements reveal some dispersion in the spectra assigned to a given minority phase, whenever different grains are examined. In particular, broad lines found in the 550–650 cm^{-1} range show a variable structure. This is probably due to a dispersion in the chemical composition of the relevant phases, in agreement with the variable compositions reported in previous works[13,17,19] [e.g., Ca_2CuO_3 (Ref. 17) and $Ca_{1.8}Sr_{0.2}CuO_3$ (Ref. 13)].

The dominant spectrum of the a, b, and c ceramics is reproduced in Fig. 6. In each ceramic, scanning from point to point only induces minor variations in this spectrum, with the exception of the line at $\sim$620 cm^{-1} whose intensity varies pronouncedly. This variation has already been noted by Cardona *et al.*[14] For the sake of comparison, the spectrum of the investigated single crystal has also been reproduced in Fig. 6.

It appears clearly in Fig. 6 that the spectra of the three ceramics are almost identical. These spectra display unambiguously the line at 280–300 cm^{-1}. This confirms the correct assignment of this frequency to the basic spectrum of the (2:2:1:2) phase in accordance with Ref. 14,

TABLE II. Most intense lines assigned to the spectra of impurity phases detected in ceramics containing as dominant phases the (2:2:1:2) and (2:2:2:3) phases. (s) and (b) denote, respectively, the sharp and the broad lines.

Minority phase composition	Main Raman lines Ref. 13	Present work
$Bi_2CaSr_3O_x$	90	93(s)
	(525)	(526)
	620	611(b)
$Ca_{0.6}Sr_{0.4}Cu_{1.75}O_3$	270	260-270(b)
	555	560(b)
$Ca_{1.8}Sr_{0.2}CuO_3$	300	300
Ca_2CuO_3	700	740(b)

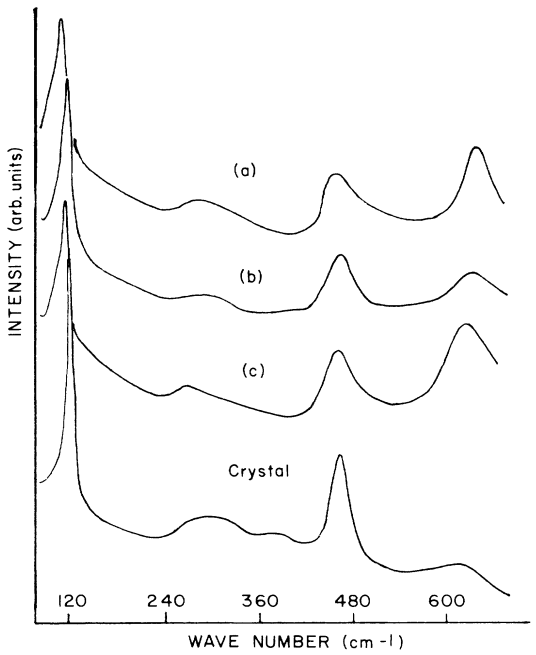

FIG. 6. Raman spectra of ceramics a, b, and c and of a single crystal of the (2:2:1:2) phase. (a) contains predominantly the (2:2:1:2) phase while (b) and (c) also contain (15–20%) of the (2:2:2:3) phase. The spectra of the ceramics have been obtained with a Raman microprobe equipped with a multichannel analyzer (incident laser power $\sim$1 mW). The single-crystal spectrum is reproduced from Fig. 2.

while our single-crystal work left some doubt in this respect.

A striking feature of the spectrum common to the ceramics, is the absence of additional lines with respect to the spectrum of the single crystal. This situation is puzzling because one expects in the ceramics a variety of scattering geometries arising from the presence of differently oriented grains. Accordingly, other lines than the ones with A_g and B_{1g} symmetries should be detected. Note that the same situation prevails in $YBa_2Cu_3O_7$ single crystals and ceramics.[18]

A first possible explanation of this situation can be ruled out; the highly oriented character of the investigated ceramics. Indeed, the Debye-Scherrer x-ray-diffraction diagrams of these ceramics yield Bragg reflections corresponding to a variety of crystallographic directions (e.g., the *a* direction and *c* direction), thus denoting a highly disoriented state. Actually, the explanation seems to reside in two features: the morphology of the grains of the superconducting phases, and their high index of refraction. One can expect that the growth habit into very thin plates, which has been observed for the (2:2:1:2) single crystals, also affects the grains of the superconducting phases within the ceramics. This is confirmed by Fig. 7 which shows a scanning electron micrograph of ceramic b. On this micrograph a number of thin plates, with various orientations, can be distinguished. These grains clearly constitute the dominant phase of the ceramic.

A light beam impinging on the ceramic will have a large probability of falling on the *c* face of a thin plate. As already explained, the high index of refraction will then cause the refracted beam to lie close to the *c* direction, whatever the incident orientation. Hence, the spectrum of a ceramic will be similar to that of *c*-oriented single-crystal plate investigated in a backscattering geometry. The fact that $YBa_2Cu_3O_7$ single crystals also grow into thin wafers[18] oriented perpendicular to *c* justifies the occurrence of the same type of situation.

Another question raised by the absence of additional lines in ceramics b and c concerns the spectrum of the (2:2:2:3) phase. This spectrum should be easily detected during the micro-Raman exploration of the ceramics since the (2:2:2:3) phase is present in ceramics b and c in a proportion of 15%–20%, much higher than that of the minority phases discussed above.

Two possible explanations can be considered. The first one refers to a previous suggestion[17] that the (2:2:2:3) phase does not constitute separate grains in a ceramic, but that is rather embedded as a crystallographic defect in the structure of the (2:2:1:2) phase. If we accept this description, the absence of a specific Raman spectrum of the (2:2:2:3) phase, in our data, results from the fact that the experiment probes a narrow layer ($\sim$1000 Å), essentially composed of the (2:2:1:2) phase, at the surface of the superconducting grains.

This picture does not seem consistent with the texture of our ceramics which were elaborated by a somewhat different procedure[16] than in previous works.[17] X-ray-powder spectra reveal, in these ceramics, Bragg reflections which are characteristic of the $\sim$37-Å *c*-lattice constant of the (2:2:2:3) phase.

The detection of such reflections seems to require the occurrence of grains of relatively large size of the (2:2:2:3) phase.

We have therefore to assume that the Raman spectrum of the (2:2:2:3) phase is effectively detected in our experiment, but that this spectrum is almost identical to that of the (2:2:1:2) phase and cannot be distinguished from it, at the present state of accuracy of the investigations. This conjecture is strongly supported by the nature of the

FIG. 7. Scanning electron micrograph of ceramic b of Fig. 6 containing the (2:2:1:2) phase and (15–20%) of the (2:2:2:3) phase.

structural differences between the two phases. As seen on Fig. 1, the atomic layers all have the same nearest-neighbor environment in the two phases. Many layers (e.g., those containing Bi and Sr) even have the same second to fourth nearest neighbors. Only the calcium layers and the additional copper-oxygen layers have different second-nearest-neighbor environments in the two phases.

Hence, if the frequencies of the modes are essentially determined by short-range forces (which is likely, except for the low-frequency modes, not apparent in the ceramic spectra) there should be a negligible shift of frequency between the modes of the two considered phases.

Besides, it is clear from the above analysis of the structures that the Raman activation of the calcium-motion in the (2:2:2:3) phase should lead to a line of small intensity since this intensity is determined by an asymmetry of the calcium site bearing on the second-nearest-neighbor only.

As for the additional copper-oxygen layer, we have already pointed out that it corresponds to the Raman-inactive lines.

The conjectured identity of Raman spectra of the different structures which are encountered within the Bi-Sr-Ca-Cu-O family is further supported by the experimental results of Cardona *et al.*[14] These authors have worked out the single-crystal spectrum of the compound $Bi_2SrCaCuO_{6+x}$. This spectrum appears almost identical to the spectrum discussed here for the (2:2:1:2) phase.

In conclusion, we have shown that the Raman spectrum of the single crystals of the (2:2:1:2) phase and of ceramics of the (2:2:1:2) and (2:2:2:3) phases can be satisfactorily interpreted within the simplified structural model of Fig. 1. No Fano effect as obvious as the one observed in $YBa_2Cu_3O_7$ has been found in the (2:2:1:2) phase. Another major difference between the spectra of these two classes of high-T_c superconductors is the occurrence in the (2:2:1:2) phases of several low-frequency modes. This calls attention to the possible existence of soft modes. Preliminary investigation of the spectra at 77 K has shown no significant temperature dependence of the various frequencies.

Finally, it is worth pointing out that, up to now, in the (1:2:3) as well as in the (2:2:1:2) compound, Raman scattering experiments have only given access, due to experimental difficulties, to atomic oscillations polarized along the *c* direction, i.e., in a direction perpendicular to the two-dimensional structural elements which are conjectured to determine the superconductivity. More interesting information would probably be obtained if one could probe the modes polarized in the *a-b* direction.

We are pleased to thank Serge Aubry for helpful discussions. One of us (H.B.) is grateful to Dr. Hadjiev for sending a copy of his work prior to publication.

[1]R. J. Hemley and H. K. Mao, Phys. Rev. Lett. **58**, 2340 (1987).

[2]G. A. Kourouklis, A. Jayaraman, B. Batlogg, R. J. Cava, M. Stavola, D. M. Krol, E. A. Rietman, and L. F. Schneemeyer, Phys. Rev. B **36**, 8320 (1987); A. Mascarenhas, S. Geller, L. C. Xu, H. Katayama-Yoshida, J. I. Pankove, and S. K. Deb, Appl. Phys. Lett. **52**, 242 (1988); G. Burns, F. H. Dacol, P. Freitas, T. S. Plaskett, and W. König, Solid State Commun. **64**, 471 (1987).

[3]M. Stavola, D. M. Krol, W. Weber, S. A. Sunshine, A. Jayaraman, G. A. Kourouklis, R. J. Cava, and E. A. Rietman, Phys. Rev. B **36**, 850 (1987); N. F. Wright and W. H. Butler, in *Proceedings of the Symposium High-Temperature Superconductors II,* edited by D. W. Capone, II, W. H. Butler, B. Batlogg, and C. W. Chu (Materials Research Society, Pittsburgh, 1988), Vol. EA-14, p. 25.

[4]C. Thomsen, M. Cardona, B. Gegenheimer, R. Liu, and A. Simon, Phys. Rev. B **37**, 9860 (1988).

[5]M. S. Zhang, C. Qiang, S. Dakun, J. Rong-fu, Q. Zheng-hao, Y. Zheng, and J. F. Scott, Solid State Commun. **65**, 487 (1988).

[6]S. L. Cooper, M. V. Klein, B. G. Pazol, J. P. Rice, and D. M. Ginzberg, Phys. Rev. B **37**, 5920 (1988).

[7]H. Maeda, Y. Tanaka, M. Fukutomi, and T. Asano, Jpn. J. Appl. Phys. **27**, L209 (1988).

[8]J. M. Tarascon, Y. Le Page, P. Barboux, B. G. Bagley, L. H. Greene, W. R. McKinnon, G. W. Hull, M. Giroud, and D. M. Hwang, Phys. Rev. B **37**, 9382 (1988).

[9]P. Bordet, J. J. Capponi, C. Chaillout, J. Chenavas, A. W. Hewat, E. A. Hewat, J. L. Hadeau, M. Marezio, J. L. Tholence, and D. Tranqui, in *High Temperature Superconductivity,* edited by J. Müller and J. L. Olsen (North-Holland, Amsterdam, 1988), p. 623.

[10]T. Kajitani, K. Kusaba, M. Kikuchi, N. Kobayashi, T. Syono, T. B. Williams, and M. Hirabayashi, Jpn. J. Appl. Phys. **27**, L587 (1988).

[11]N. Kijima, H. Endo, J. Tsuchiya, A. Sumiyama, M. Mizuno, and Y. Oguri, Jpn. J. Appl. Phys. **27**, L821 (1988).

[12]Z. V. Popovic, C. Thomsen, M. Cardona, R. Liu, G. Stanisic, R. Kremer, and W. König, Solid State Commun. **66**, 965 (1988).

[13]V. G. Hadjiev and M. N. Iliev, *Proceedings of the Eleventh International Conference on Raman Spectroscopy, London, 1988,* edited by R. J. H. Clark and D. A. Long (Wiley, New York, 1988), p. 1009.

[14]M. Cardona, C. Thomsen, R. Liu, H. G. Von Schnering, M. Hartweg, Y. F. Yan, and Z. X. Zhao, Solid State Commun. **66**, 1225 (1988).

[15]L. A. Farrow, L. H. Greene, J. M. Tarascon, P. A. Morris, W. A. Bonner, and G. W. Hull, Phys. Rev. B **38**, 752 (1988).

[16]L. Pierre, D. Morin, J. Schneck, J. C. Tolédano, J. Primot, C. Daguet, G. Glas, J. Etrillard, and H. Savary, Solid State Commun. (to be published).

[17]J. M. Tarascon, Y. Le Page, L. H. Greene, B. G. Bagley, P. Barboux, D. M. Hwang, G. W. Hull, W. R. McKinnon, and M. Giroud (unpublished).

[18]H. Savary, L. Pierre, J. Schneck, J. Sapriel, and J. C. Tolédano, in *High Temperature Superconductors,* edited by J. Müller and J. L. Olsen (North-Holland, Amsterdam, 1988), p. 419.

[19]R. M. Hazen, C. T. Prewitt, R. J. Angel, N. L. Ross, L. W. Finger, C. G. Hadidiakos, D. R. Veblen, P. J. Heaney, P. H. Hor, R. L. Meng, Y. Y. Sun, Y. Q. Wang, Y. Y. Xue, Z. H. Huang, L. Gao, J. Bechtold, and C. W. Chu, Phys. Rev. Lett. **60**, 1174 (1988).

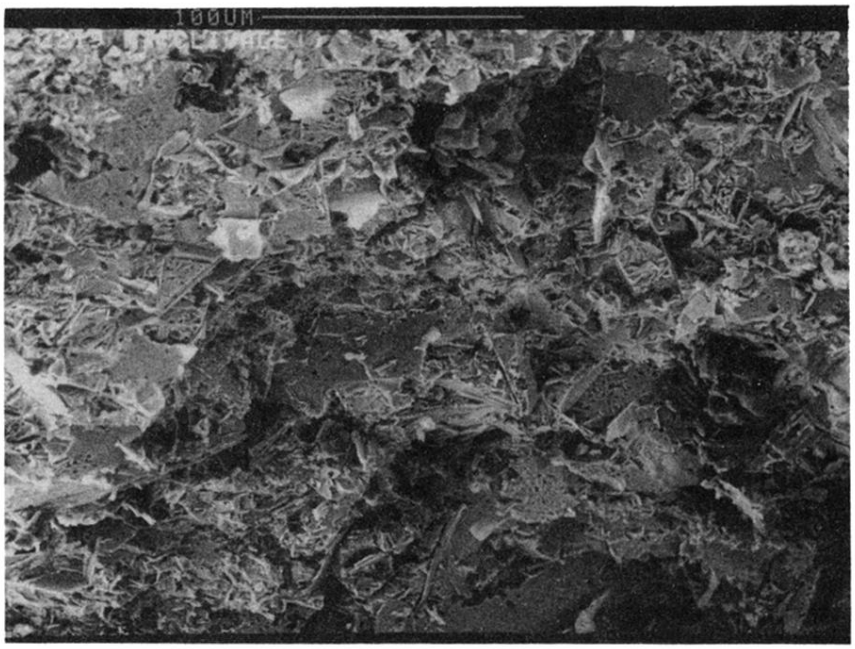

FIG. 7. Scanning electron micrograph of ceramic b of Fig. 6 containing the (2:2:1:2) phase and (15–20%) of the (2:2:2:3) phase.